American Journal of Polymer Science & Engineering
http://www.ivyunion.org/index.php/ajpse/

Research Article

Synthesis and Characterization of Novel Nanobifiller filled Epoxy Anti-Corrosive Nano-Organic coating for High Performance Automotive Applications

Sagheer Gul[1,2*], Ayesha Kausar[1], Bakhtiar Muhammad[2,], Saira Jabeen[2], Muhammad Farooq[3], and Muhammad Kashif[3]

[1] National Center for Physics Islamabad, Pakistan
[2] Hazara University, Mansehra, Pakistan
[3] Government Post graduate College, Mansehra, Pakistan

Abstract

Nanobifiller filled epoxy, nylon 66 (PA 66) and their blend-based nanocomposites were prepared by solution casting method to produce anti-corrosive and abrasion resistant epoxy nanocoating for aerospace and automotive applications. Nanobifiller was composed of Bentonite clay modified organically with quaternary salt of threonine amino acid and nanodiamonds (ND). Various techniques were implied to investigate anticorrosive properties of polymeric nanocomposites. These techniques include salt spray analysis and electrochemical impedance spectroscopy (EIS). It was observed that epoxy nanocomposites prepared are much resistant to corrosion as compared to pristine epoxy samples with improved barrier properties.

Keywords: Nanobifiller; Nanocomposite; Nanocoating; Bentonite; Nanodiamonds
Received: March 13, 2018; **Accepted**: April 16, 2018; P**ublished**: April 20, 2018
Competing Interests: The authors have declared that no competing interests exist.

***Correspondence to:** Sagheer Gul, National Center for Physics, Islamabad, Pakistan
E-mail: gul073591@gmail.com

1. Introduction

Corrosion is an immensely disastrous phenomenon which results in severe loss to economy by destroying metals, alloys and variety of composites [1]. To overcome this phenomenon various practices have been utilized with the advent of time. One such approach to seize down the phenomenon of corrosion is to take help from nanotechnology. Nanotechnology is an ever-changing field of research where researchers illustrate the preparation and properties of variety nanoparticles, nanofillers and their nanocomposites. One such interesting field dealing with nanotechnology is preparation of polymeric nanocomposite, which has revolutionized the modern day industrial products in the last few decades. In normal practice addition of low loading of some specific nanofiller in the polymer matrix is achieved through various methods and nanocomposites are generated with better properties then the pristine polymers [2]. Various types of inorganic and organic nanofillers have been incorporated in the pristine polymers and their blends at different loadings in order to study improved properties of nanocomposites [3-5]. Similarly, a variety of polymer matrices have been used for engulfing these nanofillers, of which epoxy/PA 66 blends have much attracted researchers and got worldwide attention. This is because of some remarkable properties of these nanocomposites like better tensile strength, flame retardancy, low permeability to small molecules and thermal properties compared to pure components [6].

A very interesting and recently investigated class of nanomaterial used to produce nanocomposites is nanodiamond (ND) with particle size of 2-8 nm only. These nanoparticles not only possess diamond like properties of hardness, chemical inertness and strength but also have the characteristics like conventional nanoparticles such as high surface to volume ratio, minute size and high adsorption capacity. Use of nanodiamonds as nanomaterial in production of nanocomposites has disclosed many advanced combinations of properties in electrochemical coatings, imaging probes, drug delivery systems, biosensors and lubricating systems [7,8]. However, one factor which limits the use of ND as nanofiller is its inert surface without any functional groups to interact with polymer matrix. To solve this problem a variety of active functional groups like –COOH, -NH_2, -OH etc can be easily grafted on ND surface to make it more compatible with the polymer matrix [9].

In the recent few years' different approaches have been used for preparation of nanocomposites like polymer matrix filled with more than one type of nanofiller at a time. The addition of these nanobifillers in polymer matrices leads to more pronounced properties of nanocomposites due to different interactions of two different nanofillers with the polymer [10]. Enhancement of properties by addition of these nanomaterials is generally attributed to development of much better molecular interactions between them and polymer matrix. The key to these interactions is ultimately the large surface to volume ratio of nanofillers which provides greater surface for interaction [9]. To obtain nanocomposites with high performance and better properties homogeneous dispersion of nanobifiller into the polymer matrix is also vital. A Solution induced method was practiced achieving enhancement

in thermal and mechanical properties of silicon rubber by dispersing multiwalled carbon nanotubes (MWCNTs) and grapheme (G) [11]. Various other approaches using different combinations of nanobifillers have been practised in different polymer matrices. These nanobifillers includes graphene nanoparticles (GNP)/Carbon nanotubes (CNT), nanodiamonds (ND)/CNT, CNT/ SiC and CNT/Al_2O_3 dispersed in a variety of polymer matrices to achieve different goals [12,13].

The present work describes the use of another interesting combination of nanofillers to be introduced as nanobifiller for production of epoxy/PA 66 based nanobifiller polymeric nanocomposites (Epoxy/PA/OB-ND). The nanofillers used are organically modified layered silicate Bentonite nanoclay (OB) and Nanodiamonds (ND), which have never been investigated earlier.

2. Experimental

2.1. Materials

The polymers, nanofillers and solvents were purchased from standard chemical suppliers and were used in their original form without further purification. Thermoset epoxy resin under chemical name diglycidyl ether of bisphenol-A (DGEBA) with density of 1.08 g cm^{-3} and percentage purity of 95 % was supplied by Sigma Aldrich. Commercial Nylon 66 available with chemical name of Polyamide 66 (PA 66) in form of pellets with molar mass of 262.35 g/mol and glass transition temperature (Tg) of 50^{o}C was purchased from Sigma Aldrich. The melting point of PA 66 was recorded as 255^{o}C. Formic acid used here as a solvent with 95 % purity and density of 1.2 g cm^{-3} was supplied by Sigma Aldrich. Another important solvent used in this research work was p-Cresol obtained from Fluka Chemical Corporation with 99 % purity and density of 1.034 g cm^{-3}. Commercially available Bentonite was purchased from Sigma Aldrich CAS no 1302-78-9. Amino acid Threonine used as organic modifier for Bentonite was obtained from local market with 100 % purity. Nanodiamonds (ND) with 2 nm particle size were purchased from local market Cathay Chemical works Taiwan. Teflon rods were also purchased from the local market with 1 ft length and 60 cm diameter for preparation of multiple petri dishes mechanically. To use minimum quantity of sample the internal diameter of 30 mm and depth of 10 mm for each petri dish was maintained.

2.2. Organic modification of Bentonite

The very ist step involved in the organic modification of Bentonite nanoclay was the conversion of amino acid threonine into its quaternary ammonium salt (QA) upon treatment with HCI Fig 1. For organic modification of commercial Bentonite, 2 g of nanoclay was soaked in a mixture of 80:80 ethanol/H_2O and was stirred with 40 rpm speed using magnetic stirrer at 60^{0}C for 24 hours to increase the inter layer spacing between clay layers to amplify the chances for intercalation of modifier. Calculated amount of surface modifier as per cation exchange capacity (CEC) of Bentonite was introduced in the soaked nanoclay. The mixture of nanoclay and surface modifier was left for further 24 hr continues stirring at 60^{0}C temperature. Organoclay (OB) was recovered from the suspension using suction filtration with membrane filter paper, washed several times with ethanol-water mixture in order

to remove any traces of free chloride ions and was dried in an oven at 80 ^{o}C for 24 hr Fig 2. The dried filter cake was crushed in mortar and pestle to a fine powder.

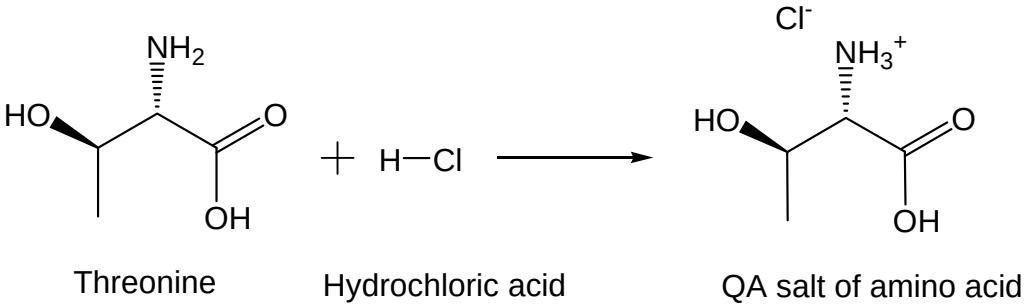

Fig. 1 QA salt formation

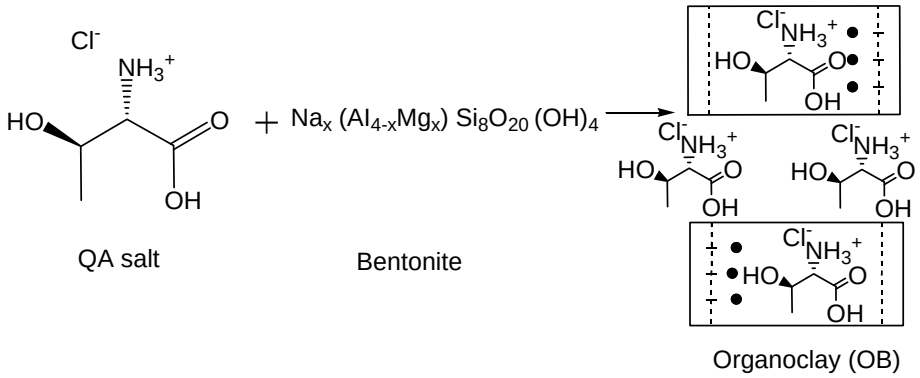

Fig. 2 Organic modification of commercial Bentonite nanoclay

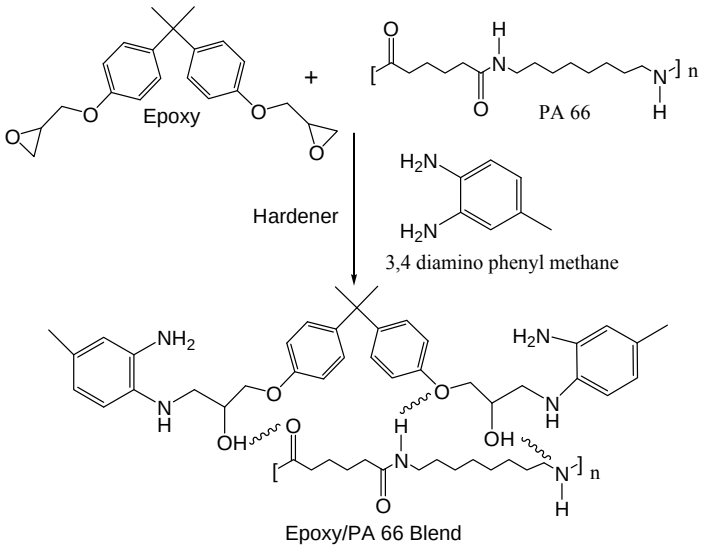

Fig. 3 Polymer blend formation

2.3. Formation of Nanoclay/Nanodiamonds (OB-ND) bifiller

For production of OB-ND bifiller 0.2 g of commercially available ND were dispersed in 10 mL of absolute ethanol through 1 hr sonication at room temperature. 1 g of OB was soaked in equimolar mixture of ethanol/water for 24 hr with continuous stirring at 60 ^{o}C. Dispersed mixture of ND was poured in OB nanoclay suspension and was placed for 4 hr reflux at 80 ^{o}C to allow maximum interaction between both nanofillers. The suspension was filtered at pump and dried in oven. Filter cake of OB-ND bifiller was crushed in mortar and pestle to finest powder to be dispersed in polymer systems for production of bifiller based nanocomposites.

2.4. Preparation of pure epoxy (Epoxy/OB-ND) and pure polyamide (PA/OB-ND) nanocomposites

Solution casting method was utilized for preparation of pure epoxy and pure PA 66 uniform thin films. For acquiring uniform epoxy thin films, a fixed amount 3g of DGEBA with different concentrations of hardener 3,4 diamino phenyl methane was practiced. After a series of unsuccessful attempts for film casting composition of 3 g of epoxy resin with 1 g of hardener was found most suitable. The mixture was stirred for 15 min at a speed of 700 rpm at room temperature until clear solution was obtained. This solution was poured in teflon petri dish and was kept in open air to stand overnight at room temperature. Uniformly hardened thin film of pure DGEBA was formed and peeled off with care and saved for further analysis. These films were dried under vacuum in an oven at 80^{o}C for 24 hrs to remive any traces of solvent. For preparation of nanocomposites various concentrations of OB-ND bifiller were dispersed in DGEBA fluid before the addition of hardener. The bifiller was given maximum possible time to be dispersed uniformly for about 20 min continuous stirring at room temperature. 1 g of hardener was then poured into this suspension and was further stirred for 15 min more for uniform interaction between DGEBA, bifiller and hardener. The final suspension was poured into teflon petri dish and was allowed to cure overnight in open air at room temperature. Bifiller was found to be dispersed uniformly throughout epoxy polymer matrix with formation of neat thin film. Epoxy/OB-ND nanocomposite film was peeled of carefully and stored for further analysis. These thin films were dried under vacuum in an oven at 80^{o}C for 24 hrs. Bifiller based nanocomposites with five different concentrations in pure epoxy polymer matrix were prepared ranging from 1 wt% to 9 wt% of the DGEBA in order to obtain comparative data for analysis. A similar procedure was adopted for preparation of PA 66 thin films by practicing 1 g of PA 66 in different solvent like dimethyl sulfoxide (DMSO), tetrahydrfuran (THF), dimethylformaide (DMF), sulphuric acid and formic acid. Formic acid was found most suitable for proper dissolution of the PA 66 giving clear solution after some time. Thus 1 g of PA 66 was dissolved in 10 mL formic acid stirred at room temperature till the clear solution was obtained. This clear solution of PA 66 was poured in glass petri dish and placed in open air at room temperature. Uniformly dried film of pure PA 66 was carefully peeled off and saved for futher analysis. These films were cured at 200^{o}C for 24 hrs. For preparation PA 66/OB-ND nanocomposites, various concentrations of bifiller ranging from 1 wt % to 9 wt% were dispersed in PA 66 solution for 20 min stirring at room temperature.

2.5. Preparation of Epoxy/PA 66 blends (Epoxy/PA)

Choice of suitable solvent is the major issue regarding preparation of thoroughly distributed thin films of blends. Once the solvent was optimized the next step was to stir both polymers together in that

solvent for a maximum period of time to get clear solution. For epoxy/PA 66 blends preparation 0.1 g of PA 66 was dissolved in 10 mL of p-cresol at 50 ^{o}C and stirred for 2 hrs. After formation of clear solution of PA 66 3 g of pure DGEBA was added in this solution and combined contents were stirred for further 40 min to allow maximum possible interactions between thermosetting epoxy and thermoplastic PA 66. PA 66 also acted as a hardening agent for epoxy to make the solution much viscous, but 1 g of hardener was mixed in above thick emulsion under 15 min stirring to produce thoroughly mixed and hardened films.

2.6. Preparation of Epoxy/PA 66/Nanobifiller nanocomposites (Epoxy/PA/OB-ND)

Epoxy/PA/OB-ND were prepared by dispersing different concentrations of OB-ND bifiller from 1 wt % to 9 wt% of epoxy in the polymer blends. The addition of bifiller was achieved just prior to addition of hardener where a clear emulsion of epoxy/PA 66 is formed. This bifiller was allowed to disperse properly under 40 min of continuous stirring at room temperature. Thin films of the Epoxy/PA/OB-ND were casted in glass petri dishes and were placed in open air to allow evaporation of solvent at room temperature. Thoroughly dried and cured thin films of Epoxy/PA/OB-ND were formed with multiple concentrations of the bifiller. These nanocomposites films were then subjected to thermal and morphological analysis to investigate the dispersion of hydrophilic OB-ND bifiller in polymer matrix.

2.7 Preparation of Epoxy bifiller nanocomposite coating

Epoxy and its blends filled with different compositions of nanobifiller were subjected to sonication for 10-12 h for thorough mixing at 60oC. For preparation of nanocoating calculated amount of hardener was added to epoxy bifiller mixtures. Nanocoating samples with different composition of bifiller (1 wt%, 3 wt%, 5 wt%, 7wt% and 9 wt %) were tested to be applied on metallic panels.

2.8 Preparation of metallic panels and applying coating

The metallic panels made of steel with dimension 8 * 4 cm were washed with kerosene oil and rubbed with sand paper to remove any traces of chemicals. These panels were dried and cleaned after which the nanocoatings were applied by suitable sized applicator. The fully coated metallic panels were dried at 25 ◦C for 120 h in open air. The dried nanofilm thickness was measured using digital micrometre screw gauge and was found to be 70ìm thick. Three thin scratches were etched on surface of these films to evaluate corrosion phenomenon after salt spray.

2.9 Characterization

Fourier transformation infrared spectrophotometer (FTIR) studies for all the samples viz pure and nanocomposites were carried out to investigate the changes in bonding interaction during synthesis of blends and bifiller filled polymeric nanocomposites. These FTIR spectra of the pure polymers, their blends, bifiller and nanocomposites were obtained using FTIR Nicolet 6700 Schimadzu, Japan. Morphological studies to investigate surface changes were carried out using Scanning electron microscopy SEM. The required SEM images at different resolutions were taken by JSM5910, JEOL, Japan. SEM analysis was mainly related to surface morphology of pristine polymers, their blends and nanocomposites. In order to study the degree of dispersion of nanobifiller in pristine polymer sand its blends. To investigate thermal properties of pristine polymers, blends and their nanocomposites thermo gravimetric analyser TGA was used. These tests were carried out using Universal V4.0C TA Instrument Q50 V6.2 Build 187 up to 800 oC with 10 oC/min rise of temperature. About 3 mg sample was sufficient for analysis taken in aluminium oxide crucible under nitrogen atmosphere flow of 50

mL/min. X-ray diffraction (XRD) patterns were obtained using a D 8 Advanced Bruker X-ray diffractometer with Cu radiation (1.54 Ao). Salt spray test was performed using ERICHSEN cupping instrument and electron impedance spectroscopy (EIS) using EG&G instrument. Tests were performed for samples with multiple concentrations of OB-ND bifiller.

3. Results and Discussion

3.1 FTIR Analysis

FTIR analysis for pristine polymers, their blends and nanocomposites were carried out to compare changes in intensities and positions of different peaks for a variety of functional groups involved Table 1. For pure epoxy Fig 4 (a), significant strong stretching band appeared at 1231 cm^{-1} for C-O ether vibrations. Bending band for substituted phenyl rings of the epoxy appeared 811 cm^{-1}. Typical umbrella deformation for methyl group of tertiary butyl was evident at 1380 cm^{-1}. Two weak bands for N-H stretch of primary amine were visible at 2922 cm^{-1} and 2858 cm^{-1} with corresponding N-H bending vibration band at 1590 cm^{-1}. These bands normally appear at higher wave numbers, however due to presence of diamine hardener amine group comes in conjugation with phenyl ring resulting in shifting of absorption peaks to lower wave numbers. Strong and broad band of hydrogen bonded alcoholic O-H Stretch appeared at 3280 cm^{-1} with corresponding C-O alcoholic stretching vibrational band at 1032 cm^{-1}. Along with these typical bands multiple bands for aromatic C=C also visible at 1508 cm^{-1}. Strong stretching vibrational band for pure PA 66 appeared at 1640 cm^{-1} due to carbonyl group of the amide linkage. Single amide N-H stretching band evident at 3300 cm^{-1} with corresponding N-H bending vibrational band at 1550 cm^{-1}. Two weak bands for N-H stretch of terminal primary amine group were visible at 2943 cm^{-1} and 2865 cm^{-1} respectively Fig 4 (b). A slight shift of absorbance towards higher wave number in these two peaks compared to N-H amine stretch of epoxy is attributed to weak intermolecular hydrogen bonding. While in case of epoxy same were linked to strong intramolecular hydrogen bonding.

Table 1 Comparative FTIR analysis

Samples	Major vibrations	Wavenumber (cm^{-1})
Pure Epoxy	C-O Stretch	1231
	O-H alcohol stretch	3280
	Substituted Phenyl bend	811
	CH_3 umbrella deformation	1380
	N-H amine bend	1590
Pure PA 66	C=O stretch	1640
	N-H stretch	3300
	N-H bending	1550
Epoxy/PA 66 blend	O-H stretch	3298
	CH_3 umbrella deformation	1380
Epoxy/PA 66/OB-ND	N-H stretch	3298
	Bentonite Si-O bands	1032

For epoxy/PA 66 blends Fig 5 (a) a combined strong and broad band for N-H stretch of amine and O-H stretch of alcohol appeared at 3298 cm^{-1}. A slight shift towards lower wave number is attributed to

hydrogen bonding of N-H and O-H groups of epoxy to that of PA 66. Two weak bands for N-H stretch of primary amine also show a delicate shift towards lower wave numbers at 2921 cm^{-1} and 2857 cm^{-1} while corresponding N-H bending vibration band elevated to 1600 cm^{-1}. These shifts clearly indicate that polymers are interacting at molecular level causing changes in original absorption shifts [14]. In formation of epoxy/PA 66/OB-ND polymeric nanocomposites the nanobifillers completely dispersed in polymer matrix losing their integrity. The uniform dispersion of OB-ND nanobifiller in epoxy/PA 66 blends results in increased interactions and decreased intensities of FTIR bands viz for N-H stretch at 3298 cm^{-1}. These increased interactions among polymers and bifillers also resulted in deformation of FTIR bands and their shift towards lower wave numbers viz N-H bend at 1586 cm^{-1}. Characteristic peak for Si-O bonds for bentonite appeared at 1032 cm^{-1} Fig 5 (b) [15].

3.2 Morphological Analysis

Detailed microanalysis of pure polymers, their blends and polymers matrices filled with nanobifiller was carried out using SEM at different possible resolution. The analysis was performed to draw a comparison between fractured surface morphology of pure polymers and their blends Fig 6. SEM analysis was further extended to investigate the effect of dispersion of nanobifiller on overall morphology of epoxy nanocomposites Fig 7, PA 66 nanocomposites Fig 8 and epoxy/PA 66/OB-ND nanocomposites Fig 10. SEM images for pure epoxy Fig 7 (a, b) provides gyroid morphology [16]. This morphology is attributed for epoxy systems due to uniform and coherent distribution of polymer molecules in respected solvent. No regions with high and low density. The presence of white regions can be attributed to presence of impurities in the amorphous polymer system [14]. Morphological analysis for pure PA 66 in Fig. 6 (c, d) shows vivid picture of polymer solution. The flake like formation which is a characteristic of high molecular weight polymers is obvious from SEM [17]. The SEM analysis of epoxy/PA 66 binary blend is shown in Fig. 6 (e, f) which reveals a large PA 66 dispersed phase domain in epoxy matrix along with few PA 66 particles pulled out of the matrix indicating poor interaction between polymers at few regions. Overall morphology for blends is uniform with maximum interfacial interaction between polymers and little non-coherence. The increased interaction between polymers is attributed to the compatibility between both polymer systems [18]. PA 66 molecules acts as successful compatibilizer for epoxy systems. For epoxy/OB-ND nanocomposites SEM analysis in Fig 7 reveals that gyroid morphology of polymer is intact with uniform distribution of nanobifiller in polymer matrix. The polymer surrounds the nanobifiller particles completely forming globules. While for PA 66/OB-ND nanocomposites Fig 8, SEM analysis reveals the pulling out mechanism of nanobifiller from polymer matrix in few regions and formation of agglomerates at many sites due to decreased interaction between polymer system and nanobifiller. These morphological results for PA 66/OB-ND corresponds to their lower thermal stability results with lowest char yield and maximum percent weight loss. SEM images obtained for epoxy/PA 66/OB-ND nanocomposites Fig 9 presents a dynamic and bright picture for dispersion of nanobifiller in binary blends. The figure presents a network morphology for nanocomposites with completely engulfed nanobifiller particles into the polymer matrix. All such morphology corresponds to the best thermal stability, better barrier and good anticorrosion properties of these nanocomposites. The good interfacial interactions between

polymers and fillers results in transfer of load to the rigid nanofiller particles which can cope with the stresses and in turn enhancement in properties is achieved [19].

3.3 Thermogravimetric analysis

Thermogravimetric analysis was carried out for pristine polymers their epoxy blends and nanocomposites to draw a comparison among their thermal stabilities. Thermograms with varying composition of nanobifiller (1 wt % - 9 wt %) were compared. Fig 11 shows a vivid comparison between thermal stabilities of nanobifiller based epoxy nanocomposites.

The thermogram in Fig 10 A(a) reveals about the thermal decomposition pattern of epoxy nanocomposite with 1 wt % of nanobifiller. The nanocomposite showed thermal stability in the range of 30-337^{o}C; with 95 % mass was conserved at this temperature. Extremely low thermal stability is attributed to the presence of very low amount of nanobifiller loading which do not sufficiently propagate into the polymer matrix with creation of very little interactions with polymer matrix. Above this temperature, a quick weight loss with decreased thermal stability of nanocomposite was observed upto 420.61^{o}C. With increasing nanobifiller percentage to 3 wt % in Fig 10 A(b) thermal stability of the sample enhanced and was experienced in the range of 30-340^{o}C; with 95 % mass of the sample was preserved at this temperature. Enhanced thermal stability of this sample was attributed to creation of strong binding interactions between nanobifiller and epoxy matrix. The OB part of the nanobifiller showed strong intermolecular interactions with organic epoxy matrix. Above this temperature there was a steady mass loss with decreased stability up to 427^{o}C. Fig 10 A(c) shows thermogram for epoxy nanocomposites with 5 wt % of nanobifiller. The nanocomposite showed further elevation in thermal stability as depicted by thermogram with stability range between 30-341^{o}C; with 94 % of the total mass of sample was retained. The increase in mass loss compared to previous sample was attributed to the creation of low and high density regions with increasing nanobifiller content. Initial decomposition of this sample starts at 341^{o}C**.** Above this temperature there is a steady mass loss with decreased thermal stability up to 417^{o}C. A similar trend was observed for the epoxy nanocomposites with increasing nanobifiller content to 7 wt % Fig 10 A(d) showed a thermal stability in the range of 30-342^{o}C; with 94 % mass of the sample was retained at this temperature. Increased thermal stability is attributed to the reinforcing effect of nanobifiller while a decrease in mass loss as compared to previous sample is attributed to the formation of some new interactions due to increased content of nanodiamonds which increases thermal stability further with retaining mass loss. Like all other samples thermal stability of this sample rapidly decreases with quick weight loss up to 463^{o}C. Similarly Epoxy nanocomposites with 9 wt % of nanobifiller Fig 10 A(e) proved to be most stable nanocomposites with thermal stability in the range of 30-344.50^{o}C; with 95 % mass of sample was conserved at 344.50^{o}C. Decomposition of this sample starts at 344.50^{o}C. The sample showed an abrupt weight loss with decreased thermal stability up to 490.6^{o}C. Fig 10 A(f) presents thermogram for pristine epoxy sample without any nanobifiller content. Extremely low stability of epoxy is evident from it with a thermal stability range between 30-111^{o}C; after which samples showed an abrupt weight loss up to 391 ^{o}C. Up till this temperature more than 90 % weight of sample is lost. In conventional nanofiller polymeric nanocomposites where by increasing nanofiller content above certain level the thermal properties used

to decrease because at high nanofiller loading a phase separation can occur between two phases with creation of low and high density regions which causes weak interactions. Unlike these conventional nanofiller polymeric nanocomposites the nanobifiller filled nanocomposites showed a further increase in thermal stability of nanocomposite with increased nanobifiller content. Which may certainly be attributed to the combined effect of both the nanofillers with increase interaction not only with the polymer matrix but also between them. These special interactions cannot be formed when dealing these nanofiller as separate entity in the polymer matrix. A similar pattern of ascending thermal stability was also achieved for nanocomposites prepared by incorporating various percentages of nanobifiller in PA 66 polymer matrix Fig 11 (a-e). The nylon matrix based nanocomposite with 9 wt % composition of nanobiffiller showed maximum thermal stability in the range of 30-396.72^{o}C; with 94.94% of the total mass was preserved at 396.72^{o}C. Above this temperature an abrupt decomposition of sample starts which limits up to 453.15^{o}C. Thermograms for nylon nanocomposites depicted extra thermal stability compared to corresponding epoxy nanocomposites due to tough nature of PA 66 compared to epoxy thermoset. Thus, tough PA 66 can absorb more energy compared to epoxy matrix. Another important factor which come into practice when dealing with nanobifiller filled PA 66 nanocomposites is the formation of strong hydrogen bonding between carboxylate groups of PA 66 and ammonium groups of the OB In addition, nanodiamonds present in nanobifiller provides extra strength to the nanocomposite acting as reinforcing agent. All of these factors collectively play important role in elevating thermal stability of PA 66 nanocomposites compared to epoxy nanocomposites. Thermograms for the nanobifiller filled epoxy/PA 66 blends were also studied using thermogravimetric analyser to draw a comparison

between their thermal stabilities with those of pristine epoxy and PA 66 nanocomposites. Nanocomposites with various composition of nanobifiller (1 wt % - 9 wt %) were prepared and tested. Thermogram for 1 wt % nanobifiller filled epoxy/PA 66 nanocomposite shown in Fig 12 (a) provides that a steady mass loss occurs in the range of 30-120^{o}C. However, the sample becomes stable between 120-340^{o}C with 94 % of the total mass retained up to this temperature. This stability is attributed to the mixing of two different polymers which results in creation of an additional intermolecular interaction between chains of the polymers which could not be achieved when the polymers are in macro size. These interactions may be strong hydrogen bonding or dipole-dipole interaction which becomes more effective at micromolecular level in solution form. Above 340^{o}C the sample showed an abrupt mass loss up to 420^{o}C due to evaporation of residual water present in hygroscopic nanocomposites. By increasing percentage composition of nanobifiller in polymer blend, the resultant nanocomposites showed an ascending trend in thermal stability. Maximum thermally stable blend-based nanocomposites were with 9 wt % loading of nanobifiller Fig 12 (e). The thermogram showed a steady mass loss between 30-240^{o}C; with 95 % of mass was conserved at this temperature. An abrupt mass loss occur between 240^{o}C-340^{o}C with 80 % mass of the sample is preserved at this temperature. A steady mass loss also occurs between 340^{o}C-440^{o}C. After 440^{o}C the sample become stable with 99 % of total mass lost Table 2. This is where the two different nanobifillers produced strong interactions with two different kinds of polymers. All such strong interactions are responsible for extremely excellent thermal stability of nanobifiller filled blends compared to pristine polymer nanocomposites.

Table 2 Comparative TGA/DTG data for nanocomposites

Samples	T_0 (^oC)	T_{10} (^oC)	T_{max} (^oC)		Char Yield (%)
			T (^oC)	Weight loss (%)	
Pure Epoxy	111	141	391	100	**-42.06**
Epoxy/OB-ND 1	337	355	420.61	85.37	**15.10**
Epoxy/OB-ND 3	340	360	427.43	85.42	**14.65**
Epoxy/OB-ND 5	341	365	417	81.20	**19.27**
Epoxy/OB-ND 7	342	349	463	84.20	**20.02**
Epoxy/OB-ND 9	344.50	351	490.6	79.98	**15.63**
PA 66/OB-ND 9	396.72	412	453.15	94.94	**5.05**
Epoxy/PA 66/OB-ND 9	440	143	440	98	**10.95**

3.4 XRD Analysis

XRD patterns of pure bentonite nanoclay and OB are compared in Fig 13 to analyse exfoliation of OB. Pure bentonite sample shows an evident reflection peak at position 2è = 5.9^o (d-spacing = 1.4 nm) is assigned to basal plane (001), which clearly agrees to interlayer spacing of nanoclay. Two small peaks for pristine bentonite at 2è = 8.8^o (d-spacing = 0.998 nm) and 2è = 9.9^o (d-spacing = 0.89 nm) are also observed which indicates the non-exfoliated behaviour of bentonite. In contrast in OB the second peak diminishes due to increase interlayer spacing of bentonite upon ionic exchange of quaternary ammonium ions within layers. The corresponding change in interlayer spacing of nanoclay is also compensated by two theta shift of the ist peak at 2è = 5.8^o (d-spacing = 1.5 nm) [20]. In Fig 14 XRD pattern of pristine nanodiamonds and OB/ND bifiller dispersion in pure polymers and their blends is shown. Pristine ND shows characteristic carbon peak at 2è = 43.6^o. The absence of basal reflection peak of OB and carbon peak of nanodiamonds in epoxy, PA 66 and their blends clearly suggests the formation of an exfoliated nanocomposites structure with uniformly dispersed bifiller.

3.5 Salt spray Analysis

This method was used to investigate the corrosion resistance of epoxy nanobifiller composite coatings using ERICHSEN cupping equipment. The water distribution highways were extended due to generation of three scratches on nanocoating films. NaCl solution 3.5 % was sprayed on these metallic panels and were exposed to salt spray for 3 weeks. Fig 15 (a-c) illustrated the visual results of samples under observation. Images clearly indicates the anti-corrosive behaviour of epoxy films compared to pure samples. The resistant of films to corrosion increases with addition of nanobifiller which reduces degradation and blistering. Best results are depicted with nanobifiller loading in epoxy/PA 66 blends due to maximum interactions between polar groups of epoxy/PA 66 and OB nanoclay. The slightly coloured thin film in Fig 15 (c) reveals almost no signs of rusting near the area of scratches with little blistering all over the surface. The results of salt spray analysis are summarized in Table 3 in accordance with ASTM B 117 standards.

Table 3 Salt spray test results with different composition of Nanobifiller.

Sample Composition	Results
Pure Epoxy	Many small blisters were formed. The surface of steel was much corroded specially near the area of scratches. Deep water penetration through the crack.
Epoxy/OB-ND 9 Wt%	A few small blisters near the area surrounding the scratches and very small portion of the total surface of steel corroded with little water penetration.
Epoxy/PA 66/OB-ND 9 Wt %	No signs of corrosion specially near the area of scratches.

Table 4 Log Z values before immersion and after T time

Sample Composition	Log Z before immersion	Log Z at time 3 weeks
Pure epoxy/PA 66	4.85	2.19
1 Wt % nanobifiller	6.75	6.05
3 Wt %	8.47	8.41
5 Wt %	8.57	8.54
7 Wt %	9.68	9.08
9 Wt %	9.99	9.54

3.6 Electrochemical Impedance Spectroscopy (EIS)

EIS technique was used to measure electrical capacitance (C) and resistance polarization (R) for each of the pristine samples and their nanocomposites. The frequency range was kept in the range of 10^5 to 10^{-2} Hz using a 20-mV amplitude. The water uptake and log Z values for each of the sample was calculated from Bode curves. These log Z values are summarized in Table 4. Utilizing Brasher–Kingsbury equation the water uptake values for all samples were calculated and summarized in Table 5.

$$\text{water uptake} = \log(C_f/C_i) \log 80$$

In this equation C_f is the final value of electrical capacitance for a sample after t time of immersion while C_i refers to the initial electrical capacitance of the nanocoating at start of experiment before exposure to solution. The results obtained from these illustrations shows that increasing amount of nanobifiller in the nanocomposites decreases water uptake with minimum value of water uptake with 9 wt % of bifiller. Fig 16.

Table 5 Water uptake values for pure sample and naobifiller filled epoxy composites after exposure to salt spray for three weeks.

Sample composition	Water uptake
Pure Epoxy/PA 66	160
1 Wt % nanobifiller	60.02
3 Wt %	23.22
5 Wt %	3.222
7 Wt %	1.112
9 Wt %	1

Acknowledgements

It is acknowledged that no funding was provided either by concerned University neither was provided by any agency. All the research work was done on purely self-expense since from synthesis to characterization.

References

1. Gergely A, Pfeifer E, Bertóti I, Torok T, Kálmán E. Corrosion protection of cold-rolled steel by zinc-rich epoxy paint coatings loaded with nano-size alumina supported polypyrrole. ***Corros Sci***. 2011, 53:3486-3499
2. Dementjev AP and Maslakov KI. Chemical state of carbon atoms on a nanodiamond surface: Growth mechanism of detonation nanodiamond. ***Fuller Nanotub Car N.*** 2012, 20:594-599
3. Kevin L and White HJ. Electrical Conductivity and Fracture Behavior of Epoxy/Polyamide-12/Multiwalled Carbon Nanotube Composites. ***Polym Eng Sci.*** 2011, 51:2245-2253
4. Golru SS, Attara MM, Ramezanzadeh B. Studying the influence of nano-Al_2O_3 particles on the corrosion performance and hydrolytic degradation resistance of anepoxy/polyamide coating on AA-1050. ***Prog Org Coat.*** 2014, 77:1391-1399
5. Ramezanzadeh B, Attar MM, Farzam MA. Study on the anticorrosion performance of the epoxy–polyamide nanocomposites containing ZnO nanoparticles. ***Prog Org Coat.*** 2011, 72:410-422
6. Gul S, Kausar A, Muhammad B, Jabeen S. Research Progress on Properties and Applications of Polymer/Clay Nanocomposite. ***Polym-Plast Technol.*** 2015, 55:684-703
7. Chang IP, Hwang KC, Chiang CS. Preparation of fluorescent magnetic nanodiamond and cellular imaging. ***J Am Chem Soc.*** 2008, 130:15476-15481
8. Chao JI, Perevedentseva E, Chung PH, Liu KK, Cheng CY, Chang CC, Cheng CL. Nanometer-sized diamond particle as a probe for biolabeling. ***Biophys J.*** 2007, 93:2199-2208
9. Jabeen S, Kausar A, Muhammad B, Gul S, Farooq M. A Review on Polymeric Nanocomposites of Nanodiamond, Carbon Nanotube, and Nanobifiller: Structure, Preparation and Properties. ***Polym-Plast Technol.*** 2015, 54:1379-1409

10. Shin MK, Lee B, Kim SH, Lee JA, Spinks GM, Gambhir S, Wallace GG, et.al. Synergistic toughening of composite fibres by self-alignment of reduced grapheme oxide and carbon nanotubes. ***Nat Commun.*** 2012, 48:650-661
11. Pradhan B and Srivastava SK. Synergistic effect of three-dimensional multi-walled carbon nanotube-graphene nanofiller in enhancing the mechanical and thermal properties of high-performance silicone rubber. ***Polym Int.*** 2014, 63:1219-1228
12. Li W, He D, Bai J. The Influence of nano/micro hybrid structure on the mechanical and self-sensing properties of carbon nanotube-microparticle epoxy matrix composite. ***Compos Part A Sci Manufact.*** 2013, 54:28-36
13. Chatterjee S, Nafezarefi F, Tai NH, Schlagenhauf L, Nuesh FA, Chu BT. Size and synergy effects of nanofiller hybrids including grapheme nanoplatelets and carbon nanotubes in mechanical properties of epoxy composites. ***Carbon***. 2012, 50:5380-5386
14. Hussain ST, Abbas F, Kausar A, Khan MR. New polyaniline/polypyrrole/ polythiophene and functionalized multiwalled carbon nanotube-based nanocomposites: Layer-by-layer in situ polymerization. ***High Perform Polym.*** 2012, 25:70-78
15. Khoshniyata A, Hashemib A, Sharifa A, Aalaiea J, Duobisc. Effect of surface modification of bentonite nanoclay with polymers on its stability in an electrolyte solution. ***Polymer Science, Ser B.*** 2012, 54:61-72
16. Kibsgaard J, Chen Z, Reinecke BN, Jaramillo TF. Engineering the surface structure of MoS_2 to preferentially expose active edge sites for electrocatalysis. ***Nat Mater.*** 2012, 11:963-969
17. Muthuraaman B, Shanmugam T, Maruthamuthu P, Nasar AS. Dye-Sensitized Solar Cell Based on a Blend of Hyperbranched Poly(aryl-ether-urethane) Electrolyte with TiO2 Nanoparticles. ***J Macromol Sci A.*** 2010, 47:965-970
18. Brito GF, Agrawal P, Araújo EM., de Mélo TJ. Polylactide/Biopolyethylene Bioblends, ***Polímeros.*** 2012, 22:427-429
19. Liu C, Luo YF, Jia1 ZX, Zhong BC, Li SQ, Guo1 GC, Jia1 DM. Enhancement of mechanical properties of poly(vinyl chloride) with polymethyl methacrylate-grafted halloysite nanotube. ***Express Polym Lett.*** 2011, 5:591-603

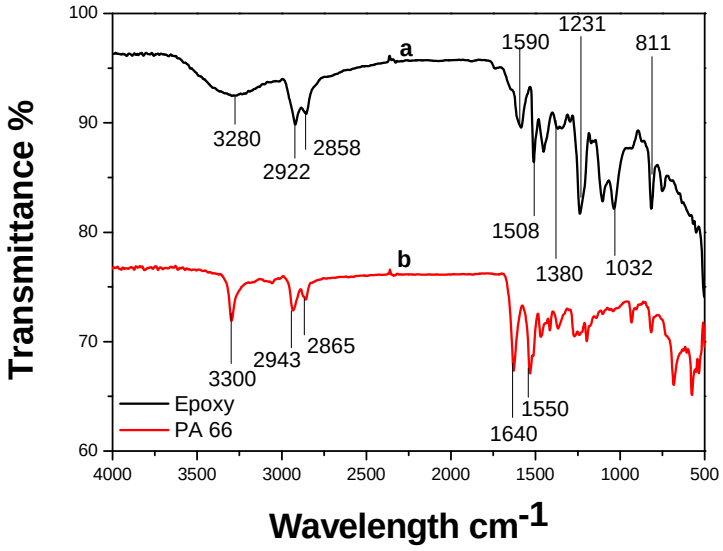

Fig. 4 Comparative FTIR analysis a) Pure Epoxy b) PA 66

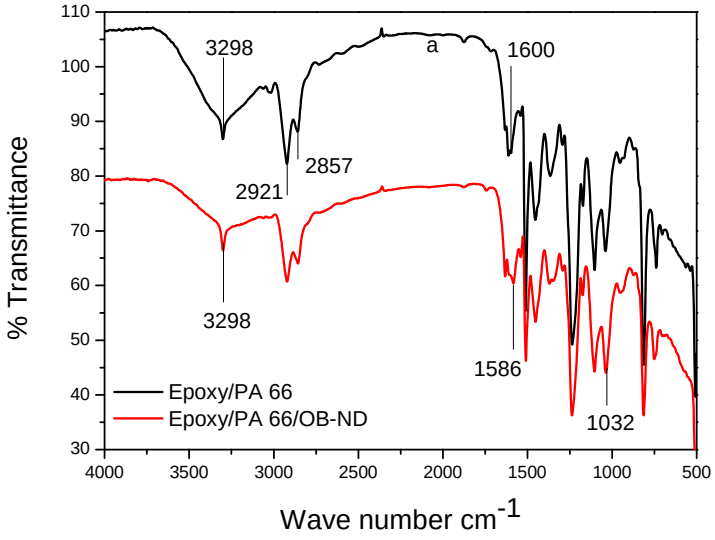

Fig. 5 FTIR spectra a) Epoxy/PA 66 b) Epoxy/PA 66/OB-ND

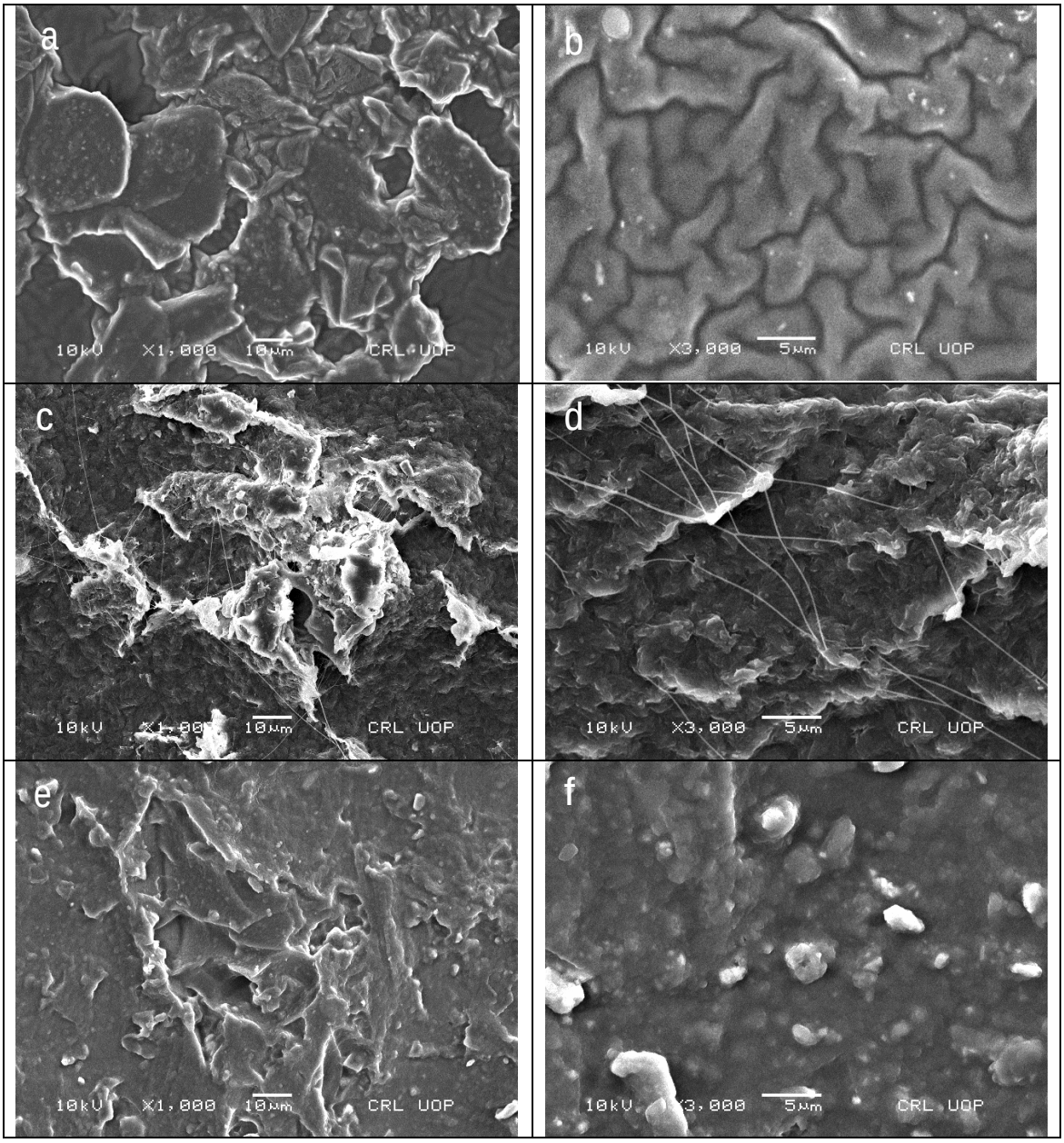

Fig. 6 SEM images of a,b) pure epoxy c,d) Pure PA 66 e,f) Epoxy/PA 66 blend

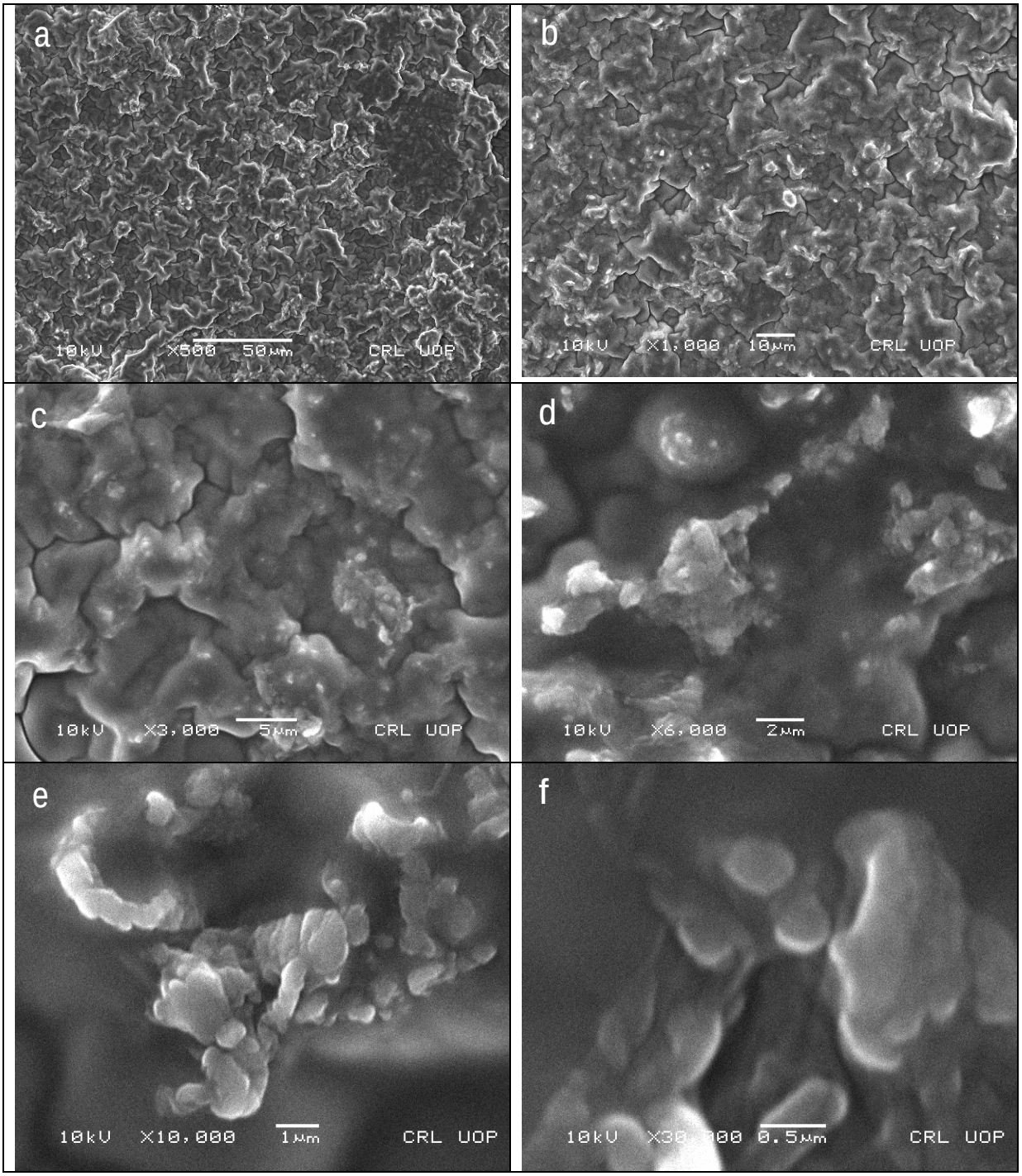

Fig. 7 SEM images of epoxy/OB-ND a) 50 ìm b) 10 ìm c) 5 ìm d) 2 ìm e) 1 ìm f) 0.5 ìm

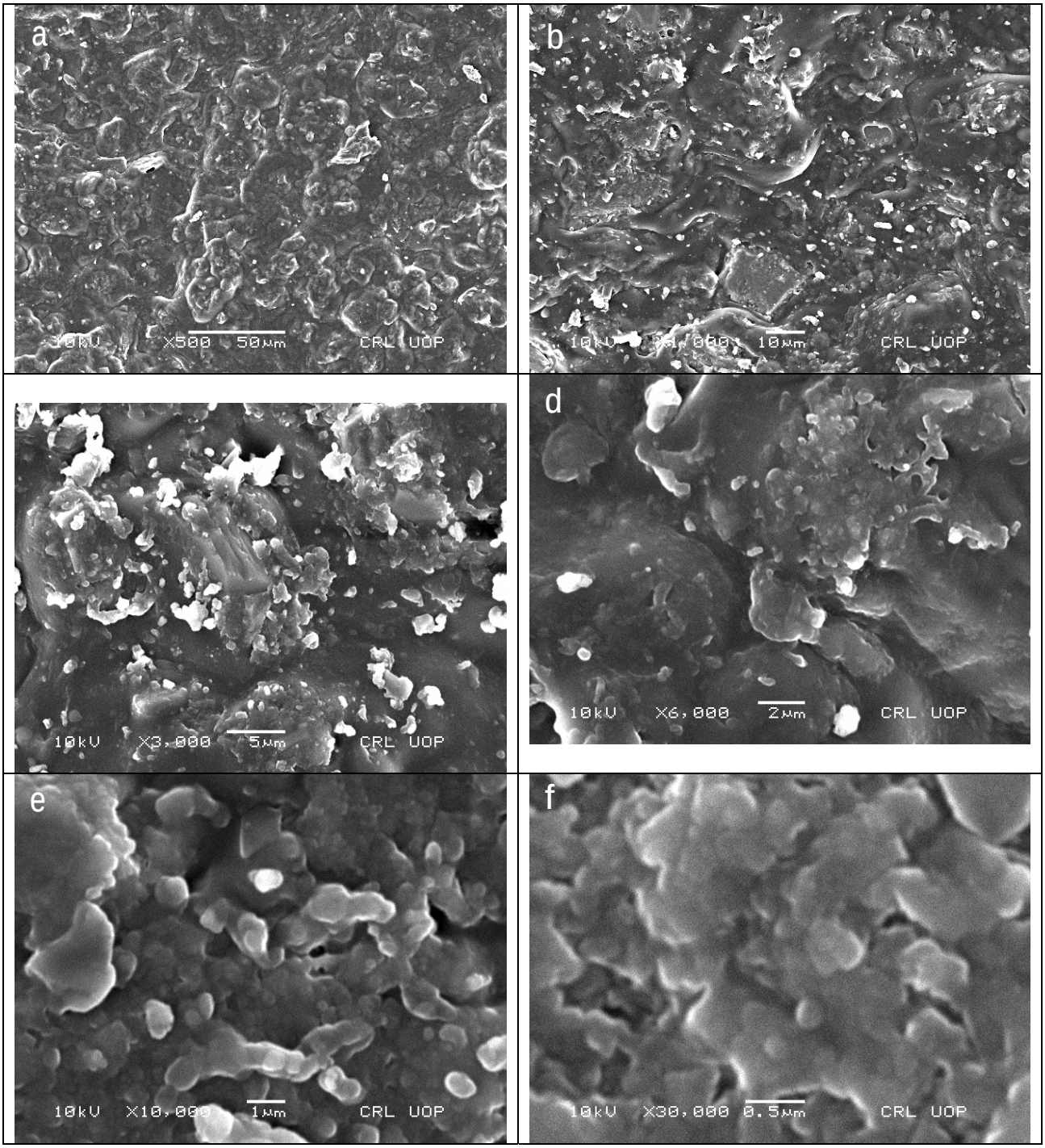

Fig. 8 SEM images of PA 66/OB-ND a) 50 ìm b) 10 ìm c) 5 ìm d) 2 ìm e) 1 ìm f) 0.5 ìm

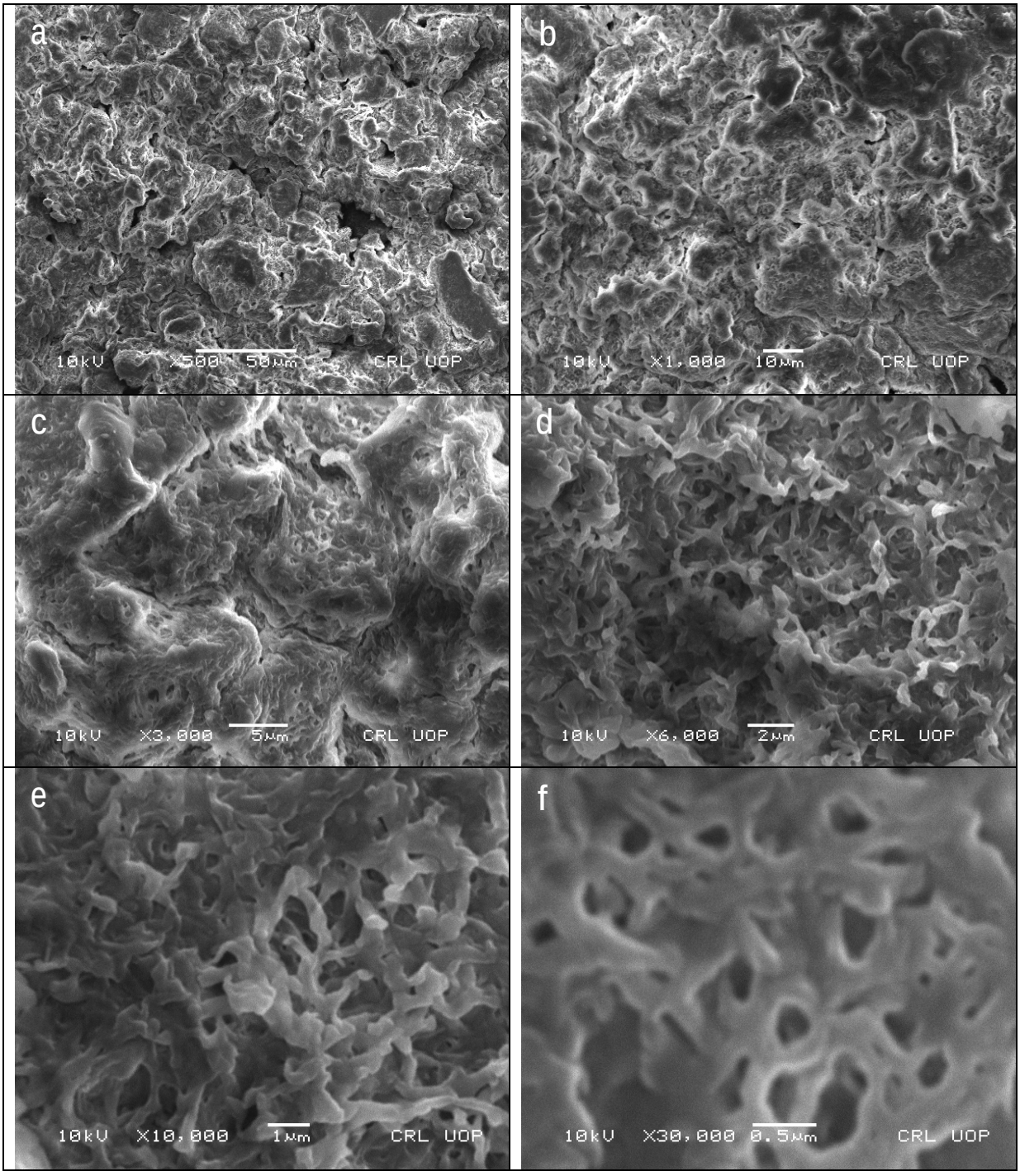

Fig. 9 SEM images of epoxy/PA 66/OB-ND a) 50 ìm b) 10 ìm c) 5 ìm d) 2 ìm e) 1ìm f) 0.5 ìm

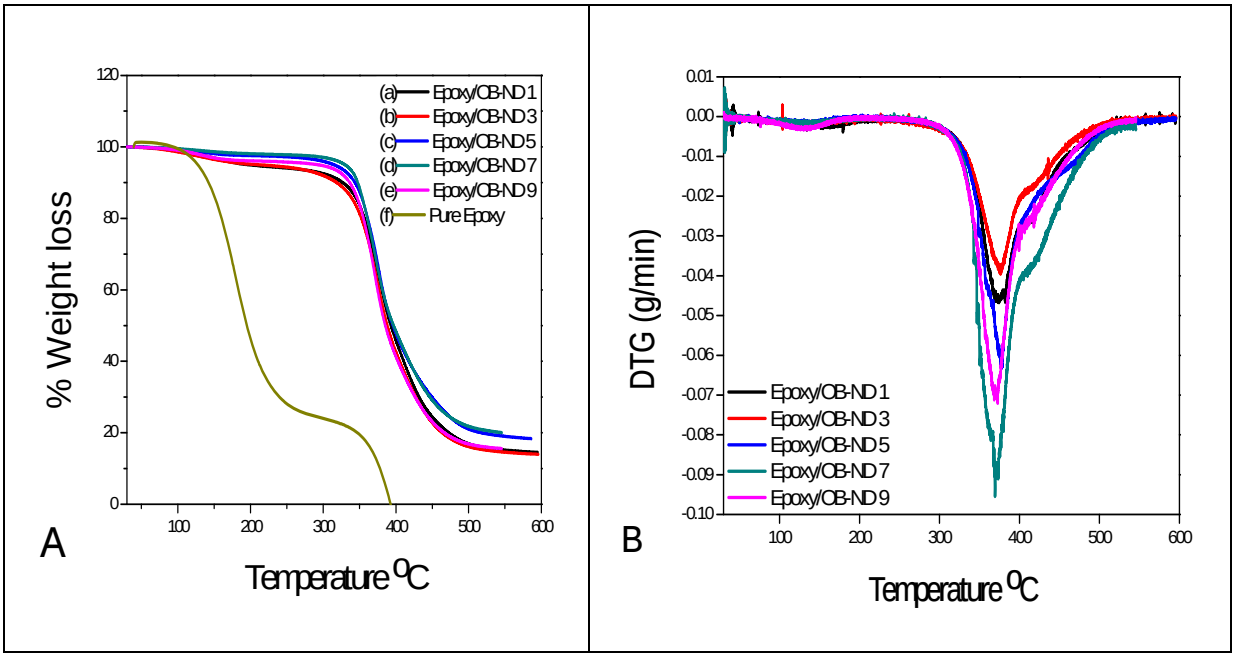

Fig. 10 TGA (A) and DTG (B) patterns of Epoxy/OB-ND nanocomposites

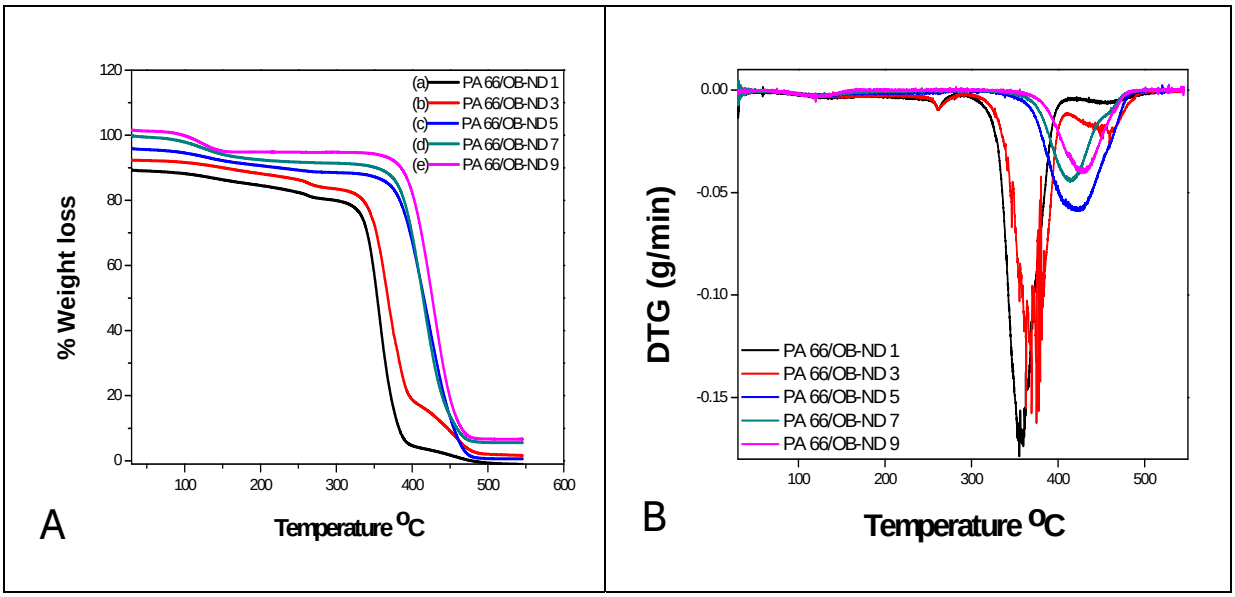

Fig.11 TGA (A) and DTG (B) pattern of PA 66/OB-ND

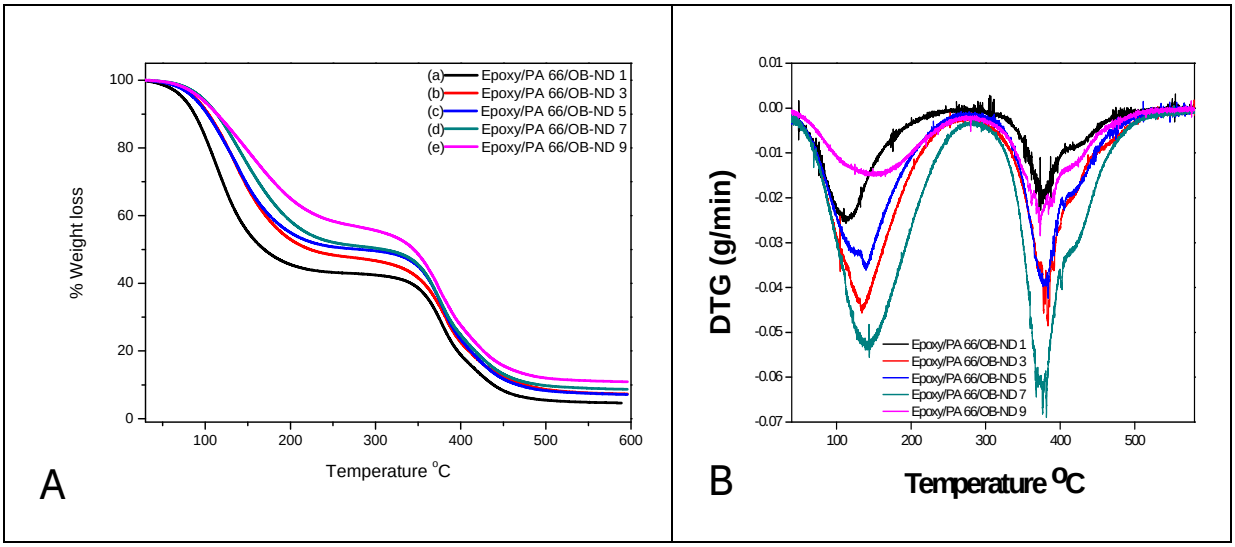

Fig. 12 TGA (A) and DTG (B) analysis of Epoxy/PA 66/OB-ND

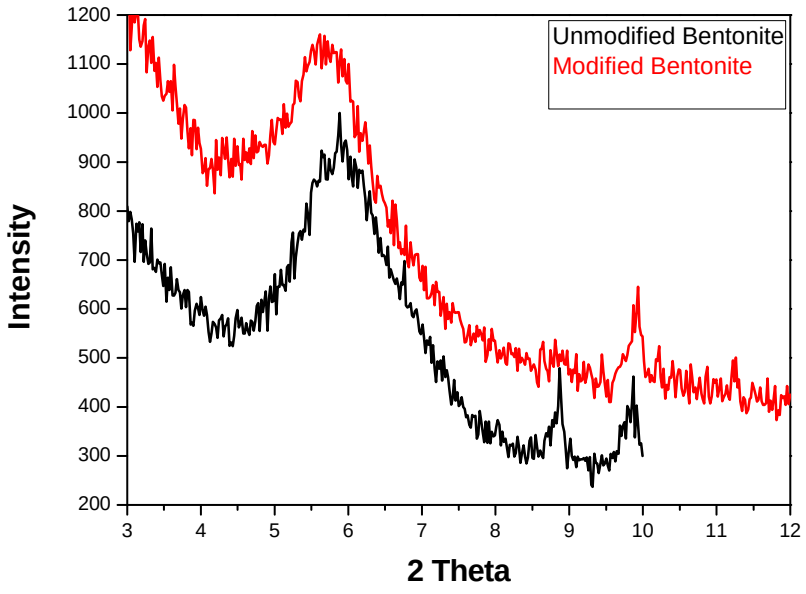

Fig. 13 XRD pattern of pure Bentonite and OB Nano clays

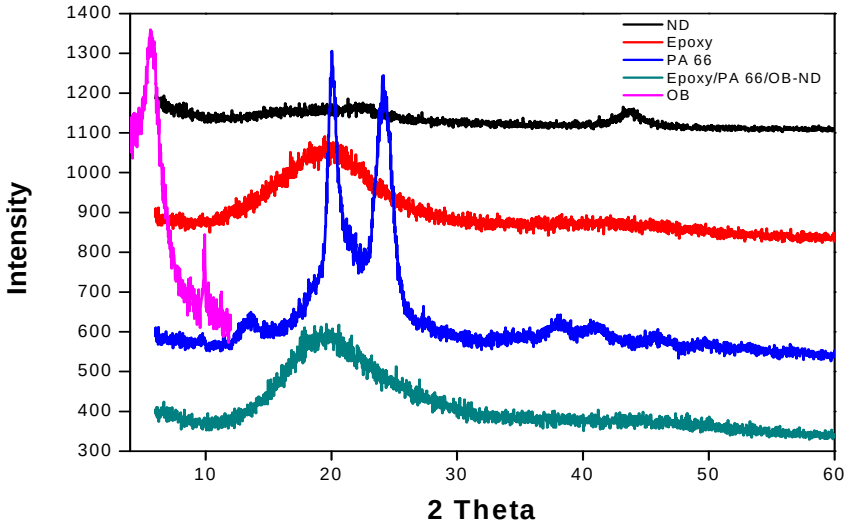

Fig. 14 XRD patterns of OB,ND and nanocomposites

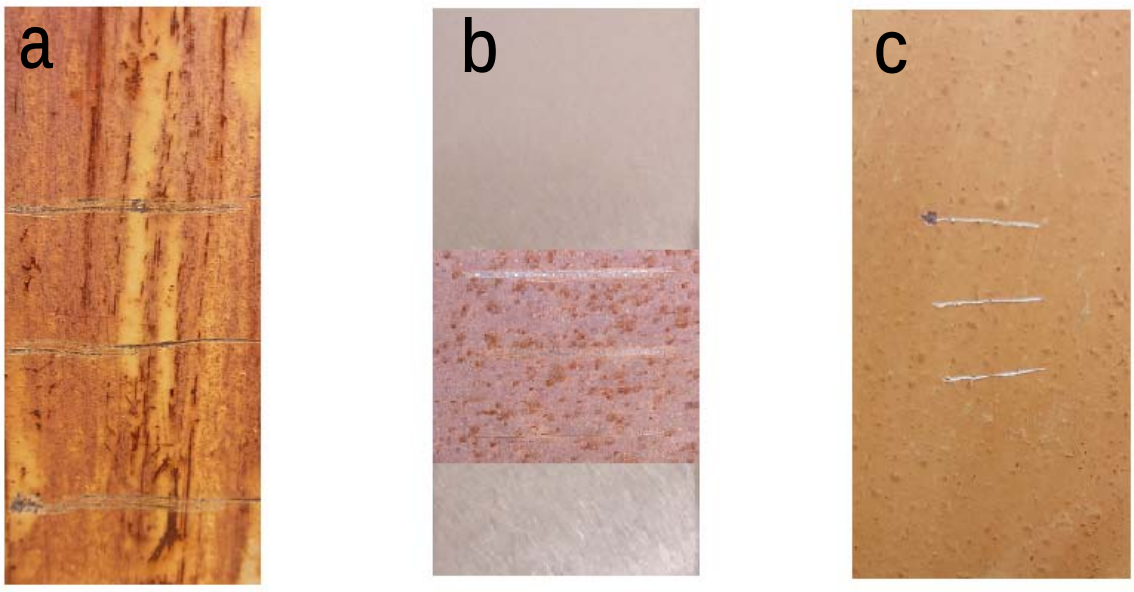

Fig. 15 Visual images of epoxy coated steel samples. a) pure epoxy b) Epoxy/OB-ND c) Epoxy/PA 66/OB-ND

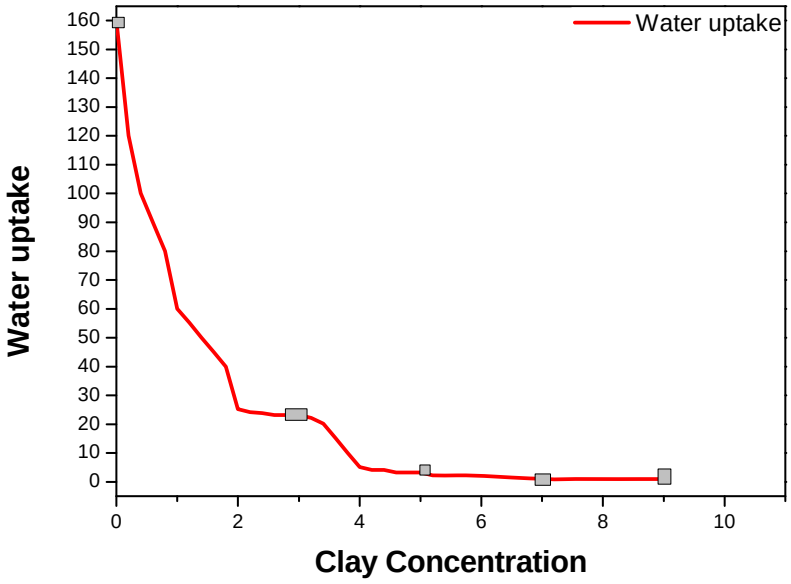

Fig. 16 Water uptake variation with changing nanobifiller concentration